Role of Multiple Intermolecular H-Bonding Interactions in Molecular Cluster of Hydroxyl-Functionalized Imidazolium Ionic Liquid: An Experimental, Topological, and Molecular Dynamics Study

Sumit Kumar Panja, Sumit Kumar, Boumediene Haddad, Abhishek R Patel, Didier Villemin, Hakkoum-Mohamed Amine, Sayantan Bera, Mansour Debdab

Article

Role of Multiple Intermolecular H-Bonding Interactions in Molecular Cluster of Hydroxyl Functionalized Imidazolium Ionic Liquid: An Experimental, Topological and Molecular Dynamics Study

Sumit Kumar Panja [1,*], Sumit Kumar [2,*], Boumediene Haddad [3,4], Abhishek R. Patel [1], Didier Villemin [4,*], Hakkoum-Mohamed Amine [4], Sayantan Bera [5] and Mansour Debdab [6]

[1] Tarsadia Institute of Chemical Science, Uka Tarsadia University, Maliba Campus, Gopal Vidyanagar, Bardoli, Mahuva Road, Surat 394350, Gujarat, India; patelabhi1120@gmail.com
[2] Department of Chemistry, Magadh University, Bodh Gaya 824234, Bihar, India
[3] Department of Chemistry, Dr. Moulay Tahar University of Saida, Saïda 20000, Algeria; haddadboumediene@yahoo.com
[4] LCMT, ENSICAEN, UMR 6507 CNRS, University of Caen, 6 bd Ml Juin, 14050 Caen, France; hakkoumamine13@gmail.com
[5] Department of Chemistry, Jadavpur University, Kolkata 700032, West Bengal, India; sayantanbera@gmail.com
[6] Laboratoire de Synthèse et Catalyse Tiaret LSCT, University of Tiaret, Algeria; mansour.debdab@univ-tiaret.dz
* Correspondence: sumitkpanja@gmail.com (S.K.P.); sumitkrmgr@gmail.com (S.K.); didier.villemin@ensicaen.fr (D.V.)

Abstract: Multiple intermolecular H-bonding interactions play pivotal role in determining the macroscopic state of ionic liquid (IL). Hence, the relationship between the microscopic and the macroscopic properties is key for a rational design of new imidazolium ILs. In the present work, we have investigated to understand how the physicochemical property of hydroxyl functionalized imidazolium-chloride related with the molecular structure and intermolecular interactions. In the isolated ion-pair, strong N-H···Cl H-bonding interaction are observed rather than observed H-bonding interactions at acidic C_2-H site and alkyl-OH···Cl of the hydroxyl functionalized imidazolium-chloride. However, N-H···Cl H-bonding interaction of the cation plays significant role in ion-pairs formation and polymeric clusters. For 3-(2-Hydroxy)-1H-imidazolium chloride (EtOHImCl), the oxygen atom (O) engages in two significant interactions within its homodimeric ion-pair cluster: N-H…O and alkyl OH…Cl. Vibrational spectroscopy and DFT calculations reveal that the chloride ion (Cl^-) forms a hydrogen bond with the C2-H group via a C2-H···Cl interaction site. Natural Bond Orbital (NBO) analysis indicates that the O-H…Cl hydrogen bonding interaction is crucial for the stability of the IL, with a second-order perturbation energy of approximately 133.8 kJ/mol. Additional computational studies using Atoms in Molecules (AIM), Non-Covalent Interaction (NCI) analysis, Electron Localization Function (ELF), and Localized Orbital Locator (LOL) provide significant insights into the properties and nature of non-covalent interactions in ILs. Ab initio molecular dynamics (AIMD) simulations of the IL demonstrate its stable states with relatively low energy values around −1680.6510 atomic units (a.u.) at both 100 fs and 400 fs timeframes due toO-H…Cl and C-H…Cl interactions.

Keywords: protic ionic liquids (PILs); ion-pair formation; H-bonding interaction; density functional theory; topological analysis; molecular dynamics

Citation: Panja, S.K.; Kumar, S.; Haddad, B.; Patel, A.R.; Villemin, D.; Amine, H.-M.; Bera, S.; Debdab, M. Role of Multiple Intermolecular H-Bonding Interactions in Molecular Cluster of Hydroxyl Functionalized Imidazolium Ionic Liquid: An Experimental, Topological and Molecular Dynamics Study. *Physchem* **2024**, *4*, x. https://doi.org/10.3390/xxxxx

Academic Editor(s): Name

Received: date
Revised: date
Accepted: date
Published: date

1. Introduction

Ionic liquids (ILs) are fascinating ionic materials that have interesting physio-chemical properties, which are helpful to prepare not only potential electrochemical devices such as fuel cells, dye sensitized solar cells, capacitors but also precursors for various chemical synthesis [1–4]. For example, the physical properties of ILs can be tailored by opting various substituents of the imidazolium ring [5]. Task-specific hydroxyl-functionalized imidazolium-based ILs have shown higher chemical and thermal stability, with well-established structural characterization, make them as a unique material for reversible capture of green-house gases [6,7], as media for organic synthesis for the enhancement of hydrophilicity and enzyme activity [8], to upgrade the solubility of inorganic salts [9], and to produce metal oxide powders with a specified size [10,11]. The polarity of task-specific hydroxyl-functionalized ILs was found to be anion-dependent and varied over a significantly wider rage due to significant different in H-bonding strength [12]. The physical and chemical properties of ILs are mainly governed by a subtle balance among various non-covalent interactions such as Coulombic interactions, H-bonding and dispersion forces [13–16]. The local and H-bonding interactions have influence on determining physical properties of IL [17,18]. Combination of cations and anions is important parameter for controlling the properties of ionic liquids [19,20]. Rational designing new class of ILs is related to macroscopic properties, can be achieved by choosing the proper composition of actions and anions related to structural parameters. However, the structure-property relationships for ILs have been systematically explored and reported by several groups [21,22]. These hydroxyl-functionalized based ILs are considered as special class of protic ionic liquids (PILs), with unique proton conducting ability used for water-free fuel cells working [23]. PILs play important role on next-generation proton exchange membrane material [24]. The proton conduction mechanism of PILs has been investigated for designing next-generation proton exchange membrane material [25,26]. According to the proton jump mechanism, PILs with multiple H-bonding interaction sites should play an important role in the enhancement of ionic conductivity and creating more efficient proton exchange membrane materials [26].

Task-specific hydroxyl-functionalized imidazolium-based ILs have shown mainly two types of H-bonding (i) involving of H-bonding interaction between a cation and an anion, and (ii) multiple ions H-bonding interactions between cation and anion. The multiple H-bonding interactions are significantly declining by presence of repulsive Coulomb forces, observed in neutral water and alcohol clusters in solution [27–29]. Recently, hydroxyl-functionalized PILs are also studied by various spectroscopic techniques and theoretical studies focused on multiple interactions in these ILs [30–32]. A variety of cations, (e.g., ammonium-, imidazolium-, pyrrolidinium-, piperidinium- and pyridinium) with an hydroxyl group were reported [33,34]. In hydroxyl-functionalized PILs, cation-cation type H-bonds might act as an important driving force for making the local structures of ILs as it compete against the repulsive Coulomb interaction between the cations and with the Coulomb enhanced cation-anion type H-bonds between cation and anion [35,36]. Precisely, FT-IR measurements mainly showed two well-defined vibrational bands that are clearly assigned to cation-anion and cation-cation type H-bonded species [36]. It is interesting to note that the H-bonding interactions between cation-cation are stronger than H-bonding interactions between cation-anion case, show the red-shifts of their corresponding vibrational bands [36–38]. Despite this expectation, however, in the bulk liquid phase, the structural motifs having H-bonded cationic clusters were mainly observed [38,39].

The present work, our aim is to understand how the physicochemical property of hydroxyl functionalized imidazolium-chloride relates the molecular structure and intermolecular interactions between anions and cations. For this purpose, FT-IR and density functional theory were applied to 3-(2-hydroxyethyl)-1*H*-imidazolium chloride (EtOHImCl; Scheme 1), which has potential applications in chemistry. Furthermore, our

goal is to explore the resemblance of theoretical results for isolated ion-pairs and small gas-phase clusters to the structures in liquid at room temperature.

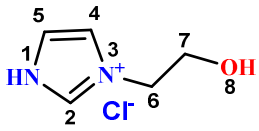

3-(2-Hydroxyethyl)-1*H*-imidazolium Chloride (EtOHImCl)

Scheme 1. Structural Formula and Abbreviation for Investigated System.

2. Experimental Section

2.1. Chemicals

All starting materials were bought from Sigma-Aldrich. These materials are of analytical grade. D_2O and $CDCl_3$ were also procured from Sigma-Aldrich and used for NMR studies. Ultrapure water, dichloromethane, acetonitrile, ethanol, DMSO, including other solvents were obtained from Sigma Aldrich.

Synthesis Procedure

EtOHImCl was synthesized from imidazole precursor according to reported procedures.[40] Firstly, reaction of imidazole (Im: 0.01 mol, 0.735 g) and 2-chloroethanol (ClEtOH: 0.67 mL, 0.01 mol) was stirred at 120 °C for 24 h. At reduced pressure, the mixture was evaporated and the obtained product was further repeatedly washed using diethyl ether (5 × 20 mL). Then the solvent was removed and product was dried under vacuum for 6 h to obtain a product with high purity. Viscous slightly yellowish liquid is obtained with a yield of 82%. The water content was measured and found to be below 360 ppm from coulometric Karl Fischer titration.

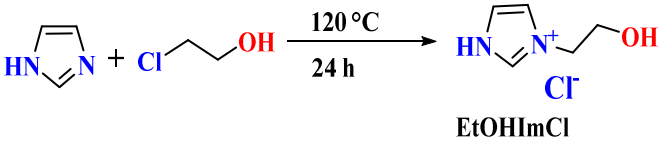

Scheme 2. Synthetic route of EtOHImCl.

2.2. Synthesis and Characterization of EtOHImCl:

Characterization of EtOHImCl IL: State: Liquid; Yield: ~82%. ^{1}H-NMR: (500 MHz, D_2O): δ (ppm) 8.91 (s, 1H, NH), 8.22 (s, 1H, C2H), 7.63 (d, *J* = 4.8 Hz, 1H, C_4H), 7.56 (d, *J* = 4.8 Hz, 1H, C5H), 4.16 (t, *J* = 4.0 Hz, 2H, -CH2-), 3.85 (t, *J* = 4.8 Hz, 2H, -CH2-), 1.99 (s, 1H, OH). ^{13}C-NMR: (150.93 MHz, D_2O): δ (ppm) 135.2, 122.0, 121.3, 56.8, 53.4.

2.3. Infrared Spectroscopy

Attenuated total reflectance Fourier transform infrared (FTIR) spectra were measured for the study of the vibrational properties. The spectra are obtained using a Vertex 70-RAM II Bruker spectrometer (Bruker Analytical, Madison, WI) operating with a Golden Gate TM diamond ATR accessory (Specac Ltd., Slough, UK). FT-IR spectra (400–4000 cm^{-1}) were collected using a nominal resolution of 1 cm^{-1} by co-adding 64 scans for each spectrum.

2.4. Quantum Chemical Calculation

2.4.1. Structure Calculations

The geometries for EtOHImCl ILs are optimized using DFT calculations applying Becke, 3-parameter, Lee-Yang-Parr (B3LYP) functional [41–43]. Further B3LYP functional

with 6-311++G(d,p) basis set was employed for predicting the most stable geometries for ILs and the interactions between cation and anion in EtOHImCl [44,45]. These geometrical optimization are performed using Gaussian 09 suite whereas the structures are visualized using Gauss View 5.1 program [46].

2.4.2. Wavenumber Calculations

FT-IR as well as Raman vibrational wavenumbers of EtOHImCl IL are calculated using B3LYP functional with 6-311++G(d,p) basis set through the Gaussian 09 program [46]. The absence of negative (imaginary) wavenumbers is monitored using Harmonic vibrational wave numbers calculation for each optimization of the structure of EtOHImCl to confirm the convergence to minima of the potential surface. The assignment of FT-IR bands is performed using VEDA program [47].

2.4.3. Binding Energy Calculation

Binding energy (BE) of EtOHImCl IL, was also separately calculated using the B3LYP functional having 6-311++G(d,p) basis set through Gaussian 09 program [46].

The binding energy for the ion-pair formation (ΔE) was measured using Equation (1), according to Turner et al. [48].

$$\Delta E = E_{AX} - E_{A^+}^{Min} - E_{X^-}^{Min} + E_{BSSE} + \Delta ZPE \quad (1)$$

where ΔE is the binding energy for the ion-pair formation whereas E_{A+}, E_{X^-} and E_{AX} are the energy of the isolated cation, anion and ionic pair respectively.

Basis Set Super-position Errors (BSSE) correction wascalculated to correct the interaction energies [49,50]. The BSSE calculation was performed using the counterpoise procedure developed by Boys and Bernardi. Further, frequency calculation provides the Zero-point energy (ZPE) correction to the interaction energy.

2.4.4. Natural Bond Orbital (NBO) Analysis

NBO analysis delivers the essential information of inter- and intra- molecular interactions [51–53]. The analysis provides the mathematical impression to acquire fundamental bonding understanding by using localized Lewis-like chemical bond [54,55]. The NBO search are formulated from the natural atomic orbital by the contribution of Natural Lewis structure [56–58]. The Lewis structure is mainly accepted when the occupancy is greater than threshold.

2.4.5. Energy Decomposition Analysis (EDA)

EDA is a computational technique used to dissect the total interaction energy between molecules or fragments of a molecular system into distinct, interpretable components. This helps in understanding the nature and contributions of various forces involved in the stability and interactions within a molecular system.

The decomposition of energy measured using quantum chemical calculations into various components having multiple chemical origin. These components are electrostatic, exchange, repulsion, polarisation, and dispersion energies. The EDA calculation is performed using GAMESS program package [59].

2.4.6. Topology Analysis

Atom-In-Molecule (AIM) analysis, Electron Localized Function (ELF) and Localized Orbital Locator (LOL) surface map analysis has been performed using Multiwfn Software Package [60]. The AIM analysis is an intuitive tool to study the electron delocalization using calculation of electron density and its Laplacian. The ELF and LOL surface maps determine the topological properties related to the probability of finding electron in atomic and molecular systems. These obeys the first-principle method for all the electrons present in the molecular system at full potential local orbitals.

2.4.7. Non-Covalent Interaction (NCI) Analysis

Non-covalent interaction analysis provides the underlying chemistry involved in various types of bonds [61]. It delivers quantitative information regarding hydrogen bond, van der Waals interaction and steric repulsion. The calculation is performed using NCIPLOT software package [61].

2.4.8. Ab Initio Molecular Dynamics Assay

Ab initio molecular dynamics (AIMD) study is performed for ILs using Orca 5.0.2 Program Package [62]. The study uses the timestep of 0.5 fs at timecon of 10 fs for 500 fs at 350 K [62]. The "timecon" parameter sets the coupling strength of the thermostat using NVT ensemble, where larger time constants correspond to weaker coupling.

3. Results and Discussion

Our aim is to establish the links between the molecular structure of the isolated ions, ion-pairs, and small clusters and the properties of the realistic condensed phase for EtOHImCl. In the current section, the results are reported based on our combined computational and experimental studies in several steps starting with the most simplistic case, i.e., isolated ion-pairs, via the more realistic situation of small clusters in the gas phase to eventually, consider the real, condense state.

3.1. Structure of Isolated Ion-Pairs and Small Clusters

To obtain the orientation patterns of the Cl^- anion and the $EtOHIm^+$ cation and its potential molecular interactions, in an isolated ion-pair and a cluster comprising of two ion-pairs are optimized at B3LYP/6-311++g(d,p) level of theory. Each optimized structure was checked to be a local minimum through normal-mode frequency calculations through the inexistence of imaginary frequencies. Initially, the cation-anion interactions were initiated by positioning the Cl^- anion near C_2-H, N-H and the hydroxyl group (-OH) of the $EtOHIm^+$ cation (Figure 1). The B3LYP method successfully is used to optimize the molecular structure (Figure 1). Interestingly, in the most stable geometry, anion is not found at the C2-H position of the cation in EtImCl, where the anion is generally located in most imidazolium-based ILs [63], and at the hydroxyl group of the $EtOHIm^+$ cation [35,64] but found to located at N-H position of cation in ion-pair of EtOHImCl IL. The most stable position of Cl^- anion is at N-H position and then the hydroxyl group (alkyl OH), least probable at C2-H position of the cation. The difference in binding energy (B.E.) with BSSE correction is 21.3 kJ/mol when the anion is positioned at the hydroxyl group (alkyl OH) site of the cation instead of the N-H site, while the difference is significantly larger, at 116.8 kJ/mol, when the anion is located at the C2-H position of the cation. These three H-bonding interaction sites make EtOHImCl a special class of PIL. Instead of H-bonding interaction between the hydroxyl group and C2-H position of the cation with Cl^- anion, the N-H…Cl H-bonding is preferable and observed for ion-pair of EtOHImCl from DFT calculation (Figure 1). The distance of C_2-H…Cl and alkyl OH…Cl is found to be 2.25 Å and 2.07 Å respectively (Figure 1b). The N-H…Cl distance is observed at 1.36 Å and the anion is preferably located on the plane of the cation (Figure 1c).

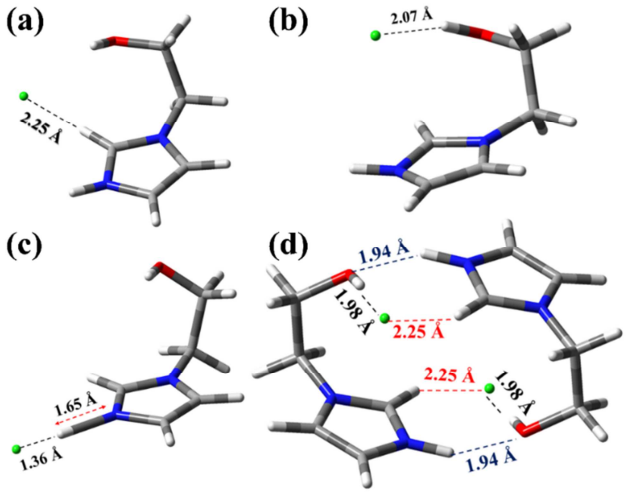

Figure 1. (**a**) C2-H…Cl (**b**) Alkyl-OH…Cl and (**c**) N-H…Cl H-bonding interactions of ion-pair in EtOHImCl. (**d**) Intermolecular Interactions of dimeric ion-pair from DFT calculation.

As aforesaid, from the calculation of ion-pairs of EtImCl, it is challenging to attain resemblance with the real material. Therefore, the next step is to increase the level of complexity by performing a small molecular cluster comprising of two ion-pairs. The most stable optimized geometry of ion-pair cluster is displayed in Figure 1d. The H-bonding between the hydroxyl group (-OH) and the chloride anion (Cl^-) can be observed at 1.98 Å in the cluster (Figure 1d). Similarly, H-bonding between the hydroxyl group (-OH) and the N-H can be observed at 1.94 Å in term of alky-O…H-N interaction in the cluster (Figure 1d). The C2-H…Cl H-bonding interaction is observed at 2.25 Å in the cluster. Interesting factor is that there are unique H-bonding sides available in ion-pair cluster via multiple H-bonding center Cl anion in both ways (Figure 1d).

In other words, this intermolecular H-bond interactions in cluster becomes stronger even in the presence of another ion-pairs. Interestingly, these twin H-bonding interactions among the hydroxyl oxygen atom associated with acidic hydrogen atom attached at the C_2 position of the other cation and Cl anion play an important role on stability of ion-pair cluster and 1D polymeric structure of EtOHImCl IL. It can be concluded that the interesting molecular interactions between reported ion-pairs are mainly dominated by cation-cation interactions and cation-anion interaction, on the other hand, do engage in further strong/directional interactions, with a cation with the other anion.

The described interactions and configuration of hydroxyalkyl group means that each hydroxyl group is involved in three H-bonds with another unit of same molecule similar to the situation often found in the alkyl alcohols and water system. Such intermolecular H-bonding interactions are identified in a small cluster rather than complex and bulky molecular systems. In the liquid state, these H-bond network exhibits dynamic behavior resulting some different bonding states. This gives rise to distinguishable vibrational frequencies manifesting as broad -OH stretching bands [38]. Furthermore, the later section of this paper focused on the discussion of the experimental vibrational spectra recorded in the solid state will shed some light.

3.2. FT-IR Studies

In order to investigate the role of vibrational modes towards intermolecular molecular interactions, FTIR measurements were carried out in solid state. Figure 2 represents the C-H/O-H stretching regions for IM (Imidazole) and ClEtOH (2-Chloroethanol) respectively. Table 1 summarizes the assignment of the experimental vibrational bands and the detailed rigorous analysis of FTIR bands is presented in the Supporting Information (see Table S3). The aliphatic C-H stretching modes is ranged from 2700 to ~3000 cm^{-1} (alkyl group), while the aromatic C-H groups vibrationsare observed at higher frequency

range between 3000 and 3200 cm^{-1} for IM (imidazole). The strong OH stretching bands are observed and located at 3366 cm^{-1} and 3569 cm^{-1} for ClEtOH (Figure 2). The OH stretching peaks is appeared at two distinct wavenumbers and indicates that the OH groups can exist in two distinct states of strongly H-bonded OH groups and free OH groups. The free OH stretching vibration of IL has shown similar spectral behaviour to the alcohols and water [38,65,66]. Interestingly, this supports that these OH groups of IL are not contributing in 1D arrangement via any intermolecular interaction. The band at 3417 cm^{-1} of EtOHImCl is close to asymmetrically H-bonded O-H of water molecules [66]. This experimental results strongly support our hypothesis that each OH group of EtO-HImCl is involved in two different H-bonding interactions [64]. These H-bonding are responsible for stability of various molecular systems [52,58,67–69].

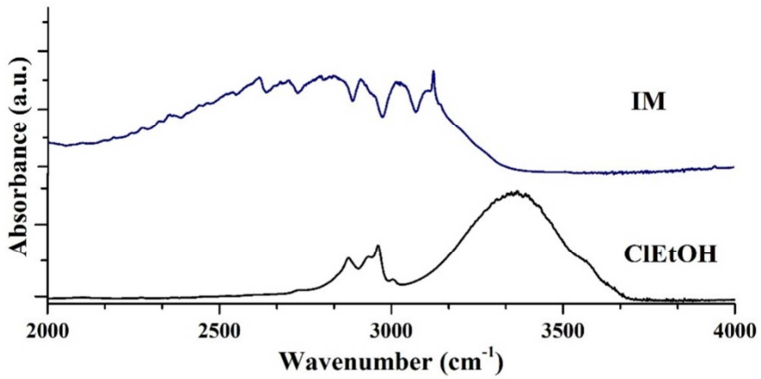

Figure 2. Experimental FTIR spectra of IM and ClEtOH (at region: 2000–4000 cm^{-1}).

Table 1. Observed FTIR bands along with their assignment.

Experimental	Vibrational Band Assignment
651	ω(N-H)/CH_3(N) CN Str
702	CH_2(N)/CH_3(N)CN bend
755	ω(N-H)
868	ring CC bend
944	$\rho_{as}(CH_2)$
1069	νC-O
1166	Ring as Str CH_2(N) and CH_3(N)CN Str/CC
1255	Ring ip as str
1338	Ring, ν(CH_2-N)
1386	δ (N-H) ip vibration
1428	δ (O-H) ip vibration
1455	δ(CH_2)/CCH, HCH as bend
1475	Str CH_2(N)/CH_2(N)CN Str
1634	Ring vibration C=C
1636	Ring vibration C=N
2882	$\nu_s(CH_2)$ as Str
2955	ν_{as} (CH_2) as Str
3095	ν(N)CH_2 as Str
3149	νC(4/5)-H str
3364	ν(N-H)/(O-H)

(ν = Str = stretch, δ = deformation, bend = bending deformation, ω = wagging, ρ = rocking, s = symmetric, as = antisymmetric; ip = in plane; op = out plane).

We systematically assign the vibrational band for our present system (EtOHImCl; Figure 3) with the help of our previous studies [30]. The stretching vibrations of the $C_{4/5}$-H groups is observed at 3151 and 3132 cm^{-1}. These vibrational frequencies are found to be slightly different chemical environment and can be observed in Figure 3. The C_2-H stretch vibration is observed at 3106 cm^{-1} due to the presence of H-bonding interaction betweenC_2-H and Cl anion. Above experimental results support that H-bonding interaction takes place between the C_2-H groups of the cations and Cl^- anion. Strong interactions between the cation C_2-H and the Cl^- anion do take place in EtOHmimCl but Cl anion is also made H-bonding interaction worth -OH group [5]. The stretching vibrational modes of the aliphatic C-H groups appeared in the region between 2800 and 3000 cm^{-1}. Interestingly, two different vibrational modes of CH_2 group are observed due to presence of the hydroxyethyl chain with chemically different environment as one is neighboring an oxygen and the other one a nitrogen atom. The vibrational mode of EtOHImCl at the fingerprint region provide the useful molecular information related to cation-anion interaction of EtOHImCl PIL. In the experimental FTIR spectrum, the vibrational mode of C=C bond is found at 1565 cm^{-1}. Interestingly, the shape of non-symmetric the vibrational mode of C=C bond is consisted of a weak shoulder at 1570 cm^{-1}.

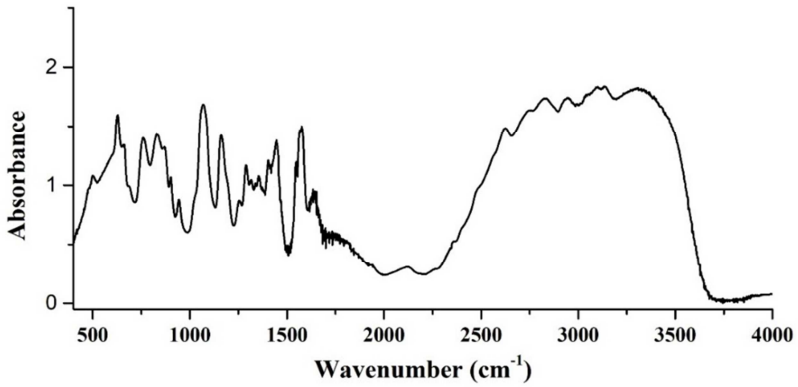

Figure 3. Experimental FTIR spectra of EtOHImCl (at region: 400–4000 cm^{-1}).

The experimental results suggested that the C_2-H group of the cation forms a H-bond along with Cl anion which is also form connected to the hydrogen atom of the alkyl hydroxyl group of another cation. The other C-H groups (aliphatic and aromatic) seemed to be not contributed in H-bonding interactions.

Further, temperature dependent FT-IR spectra is also measured in 25−80 °C temperature range (Figure 4). It is observed that there is not new vibrational band appeared in 500–4000 cm^{-1} range but intensity of spectral band is observed. With increase of temperature, the absorbance is decreasing only, no change of spectral pattern and peak position of each band. It is clear that there is no significant change intermolecular interaction up to 80 °C as no change of involved vibration modes.

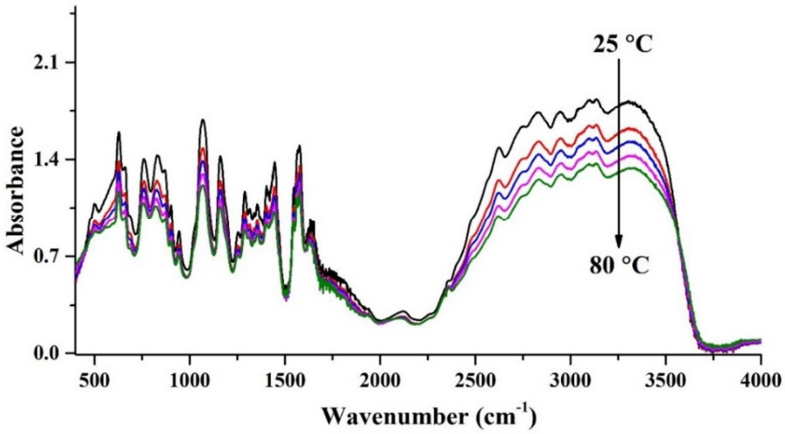

Figure 4. Temperature Dependent FTIR spectra of EtOHImCl (at region: 400–4000 cm^{-1}).

3.3. Raman Studies

In Raman spectra of EtOHImCl, very strong bands can be found in the region (1500–500 cm^{-1}). In the C-H stretch region, strong bands are also observed. The deconvoluted Raman spectra are also presented in Figure 5. Figure 5 is also fitted by using the nonlinear curve-fitting algorithm. The vibrational wavenumbers in the region 3200–2800 cm^{-1} dictates the C-H stretching vibrational modes of the imidazolium ring along with the aliphatic C-H of the alkyl chain, respectively [70]. In the region 3200–3500 cm^{-1}, vibrational modes of hydroxyl group and N-H stretching vibration are assigned from experimental and theoretical study. Therefore, Raman results provide crucial structural information of the EtOHImCl PIL. The alkyl C-H region and imidazolium ring C-H region have shown highly Raman and FT-IR active modes for EtOHImCl. Significantly strong signals are observed in the C-H stretching vibrational region due to strong Raman scattering cross section of CH groups. It is found that the C_2–H bond of the cation able to form a H-bond with the Cl anion in the form of C_2-H···Cl interaction in cluster from theoretical calculation. Therefore, the C_2–H stretching vibrational mode in imidazolium cation may provide an idea about the existence and strength of inter and intramolecular H-bonds in EtOHImCl PIL.

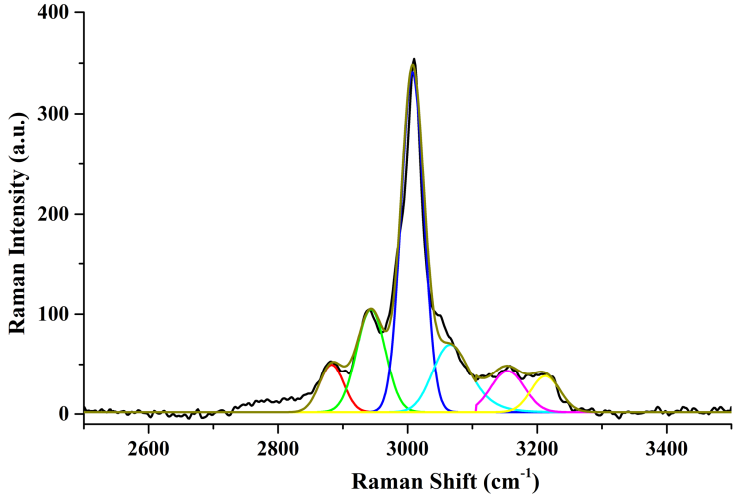

Figure 5. Experimental Raman spectra of EtOHImCl (at region: 2500–3600 cm^{-1}).

However, the interpretation of the C–H region is discussed in the previous literatures.[71,72] The C_2-H vibrational band is appeared at ~3070 cm^{-1} for ion-pair of EtOHImCl. The observed vibrational band at 3110 cm^{-1} and 3140 cm^{-1} are attributed to the C_4H and C_5H stretching modes of EtOHImCl. The observation of C_2-H stretch at 3070

cm^{-1} is lower wavenumber than $C_{4/5}H$ was explained by the strong hydrogen bond formation of C_2-H for ion-pair network. Initially, the Clanion locates at top of EtOHIm cation in momimeric ion-pair but a strong C_2-H···Cl interaction is observed in dimeric ion-pair cluster. Further, the alkyl-OH stretching mode is observed at 3020 cm^{-1} and it is also lower than C_2-H stretching vibration. Redshift of the alkyl-OH stretching is observed due to the presence of strong interaction between alkyl OH and Cl anion in EtOHImCl. The strong stretching vibrational mode of CH_2 group is observed at 2964 cm^{-1}. Further, aliphatic C-H vibrational modes are appeared at 2830–2890 cm^{-1}.

Table 2. Vibrational band assignment from experimental and theoretical studies.

Band Assignment	Experimental: Raman	Theory: Ion-Pair	Dimeric Ion-Pair Cluster
$\nu_{AS}(C_{4,5}-H)$	3140/3110	3140	3140
$\nu(C_2-H)$	3070	3171	3018
$\nu(O-H)$	3020	3125	3178
$\nu_{AS}(N-CH_2)$	2964	3021	3005
$\nu(C=C)$	1567	1590	1579

For the C-H region 3300–2700 cm^{-1}, the $C_{4,5}$-H stretching at 3140 cm^{-1} was selected as a reference peak for scaling the theoretical wavenumbers and the scaling factor is found to be 0.99 [73].

Experimental vibrational mode of C=C bond is appeared at 1567 cm^{-1} and shows that its line shape is symmetric in nature. A new vibration at 1451 cm^{-1} is assigned to CH_2 scissor and can be correlated to the 1451 cm^{-1} mode in the experimental Raman spectrum.

Two rotational isomers of the bmim cation can coexist, namely one with a trans and the other with a gauche conformation in n-butyl chain attached with imidazoliumring [35,74,75]. From experimental result, the gauche marker band exists and observed at 601 cm^{-1}, while weaker trans marker band is observed at 625 cm^{-1} (Figure 6). From the above experimental result, it is confirmed that the conformation in EtOHmim cation with Cl anion is only existed as gauche and also confirmed by DFT calculation (Figures 1 and 2). Figure 7 shows the experimental Raman spectra of EtOHImCl PIL in the region 500–3600 cm^{-1} along with scaled theoretical Raman spectra at B3LYP/6-311++G(d,p) level of theory for better understanding [73].

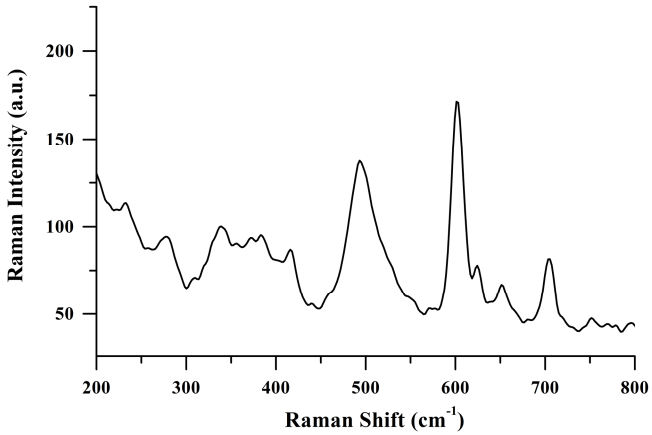

Figure 6. Low frequency Raman spectra of EtOHImCl (at region: 350–800 cm^{-1}).

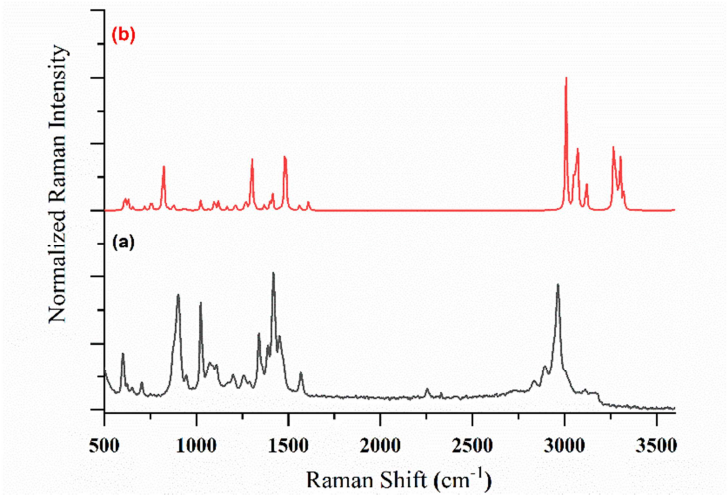

Figure 7. (**a**) Experimental and (**b**) theoretical Raman spectra of EtOHImCl (at region: 500–3600 cm^{-1}).

3.4. Natural Bond Orbital (NBO) Analysis

NBO analysis mainly depicts the molecular interaction analysis through second-order Fock matrix calculation. It is carried out for all feasible interactions between filled (donor, i) Lewis-type along with unfilled (acceptor, j) non-Lewis type NBOs [76]. The loss of occupancy occurs for the localized Lewis-type NBOs while gain of occupancy occurs for non-Lewis orbitals. The second-order Fock matrix calculation (ΔE_{ij}) is described using off diagonal NBO Fock matrix element (F(i,j)), donor orbital occupancy (q_i),diagonal elements (εj and εi). The selected NBO parameters for optimized structures of dimer of EtOHImCl IL are depicted in Table 3.

Table 3. Selected NBO parameters for optimized structures of EtOHImCl IL dimer [77]. Atom numbering is shown in Figure S2 in Supporting Information.

NAOs	Donor NBO (i)	Occupancy	NAOs	Acceptor NBO (j)	Occupancy	E(2) kJ/mol
27	n(1)O1	1.96153	106	σ*(1)N21-H34	0.03328	30.00
28	n(2)O1	1.94428	106	σ*(1)N21-H34	0.03328	5.10
30	n(1)O17	1.96158	87	σ*(1)N4-H19	0.03318	29.92
31	n(2)O17	1.94426	87	σ*(1)N4-H19	0.03318	4.94
35	n(3)Cl35	1.95316	93	σ*(1)C11-H12	0.05446	46.19
36	n(4)Cl35	1.87669	93	σ*(1)C11-H12	0.05446	15.90
33	n(1)Cl35	1.99900	98	σ*(1)O17-H18	0.10664	6.69
36	n(4)Cl35	1.87669	98	σ*(1)O17-H18	0.10664	134.31
37	n(1)Cl36	1.99900	79	σ*(1)O1-H2	0.10635	6.65
40	n(4)Cl36	1.87718	79	σ*(1)O1-H2	0.10635	134.01
39	n(3)Cl36	1.95307	112	σ*(1)C28-H29	0.05436	46.40
40	n(4)Cl36	1.87718	112	σ*(1)C28-H29	0.05436	15.61

Interesting, the NBO parameters nicely shows the interaction for various inter and intra-hydrogen bonding interactions in the ion-pair of EtOHImCl PIL.

3.5. Topology Analysis

3.5.1. AIM Analysis

The AIM analysis provides useful information regarding quantitative understanding of intra and inter-molecular interactions. The analysis uses the parameter such as electron density $\rho_{bcp}(r)$ and Laplacian of electron density $\nabla^2\rho_{bcp}$ (r) and provides the in-

formation regarding covalent and non-covalent bonding interaction [51,78]. Figure 8 shows the AIM representation of dimer of EtOHImCl PIL calculated using the structure optimized at B3LYP/6-311++G(d,p) level of theory whereas the related data has been plotted in Figure 10. The IL has been stabilized through the important H-bonding interaction such as O1-H2…Cl36, C29-H29…Cl36, C11-H12…Cl35, O17-H18…Cl35, N4-H19…O17 and N21-H34…O1. Interesting the bond critical point (BCP) has been observed between the connected atoms showing the strength of H-bonding interaction using $\rho_{bcp}(r)$ and $\nabla^2\rho_{bcp}$ (r). $\rho_{bcp}(r)$ value at the BCP between H2…Cl36, H29…Cl36, H12…Cl35, H18…Cl35, H19…O17 and H34…O1 are measured −0.0078, 0.00112, 0.00111, −0.0078, 0.00232 and 0.00231 a.u., respectively. The corresponding $\nabla^2\rho_{bcp}$ (r) value of dimer of EtOHImCl PIL 0.07218, 0.06475, 0.06475, 0.07216, 0.09144 and 0.0916 a.u., respectively.

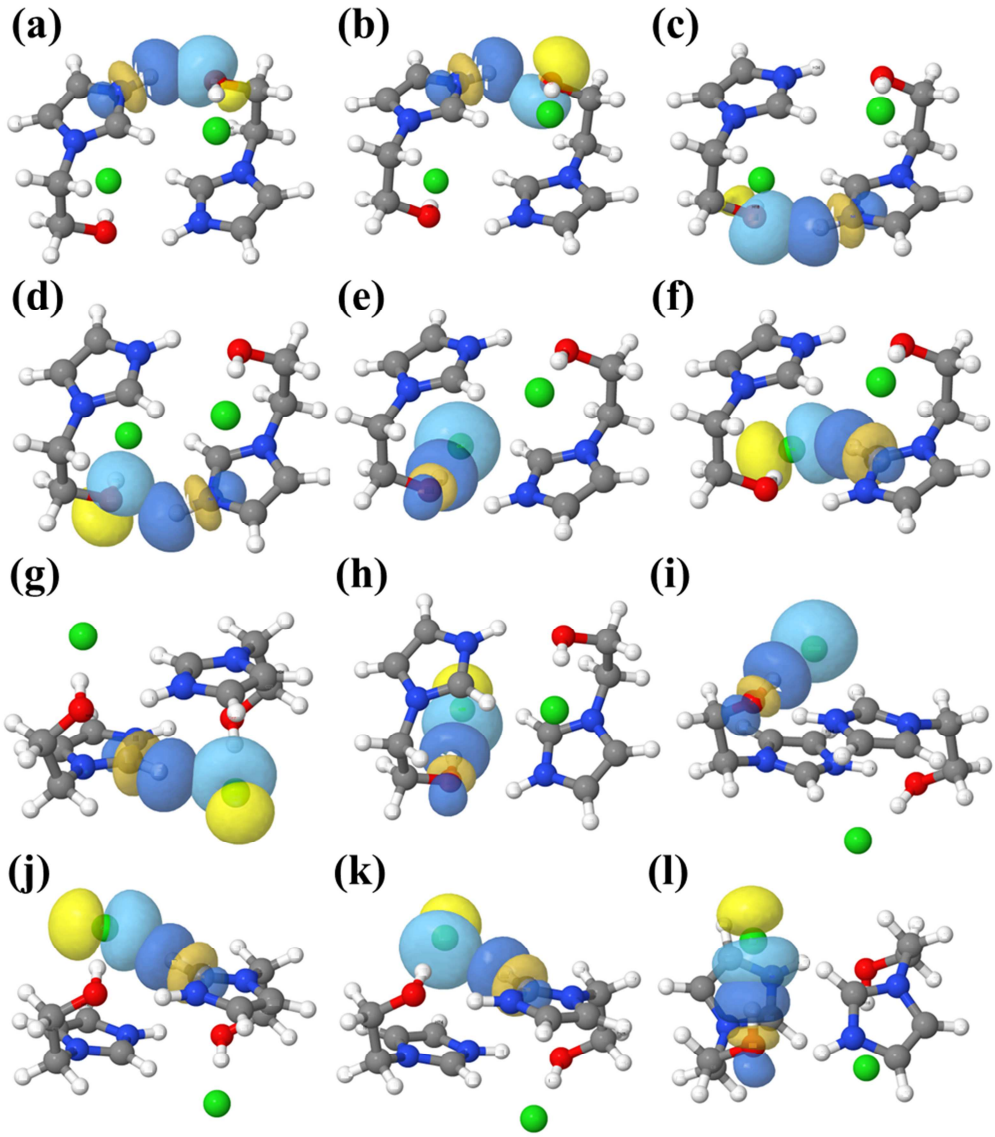

Figure 8. NBO interaction of (**a**) n(1)O1→σ*(1)N21-H34, (**b**) n(2)O1→σ*(1)N21-H34, (**c**) n(1)O17→σ*(1)N4-H19, (**d**) n(1)O17→σ*(1)N4-H19, (**e**) n(3)Cl35→σ*(1)C11-H12, (**f**) n(4)Cl35→σ*(1)C11-H12, (**g**) n(1)Cl35→σ*(1)O17-H18, (**h**) n(4)Cl35→σ*(1)O17-H18, (**i**) n(1)Cl36→σ*(1)C1-H2, (**j**) n(4)Cl36→σ*(1)C1-H2, (**k**) n(3)Cl36→σ*(1)C28-H29 and (**l**) n(4)Cl36→σ*(1)C28-H29 for EtOHImCl IL dimer. Atom numbering is shown in Figure S2 in Supporting Information.

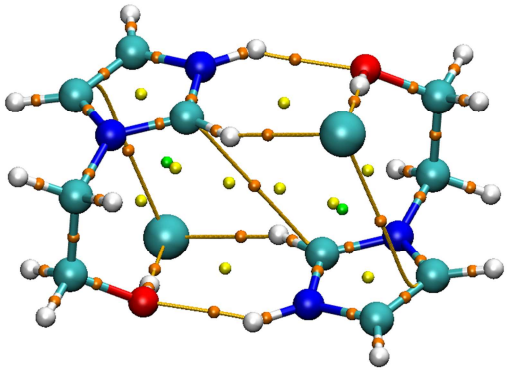

Figure 9. AIM representation of dimer of EtOHImCl PIL. Small red spheres show bond critical points (BCP) whereas path joining these spheres are bond path. Small yellow and green spheres show ring critical point (RCP) and cage critical point (CCP), respectively.

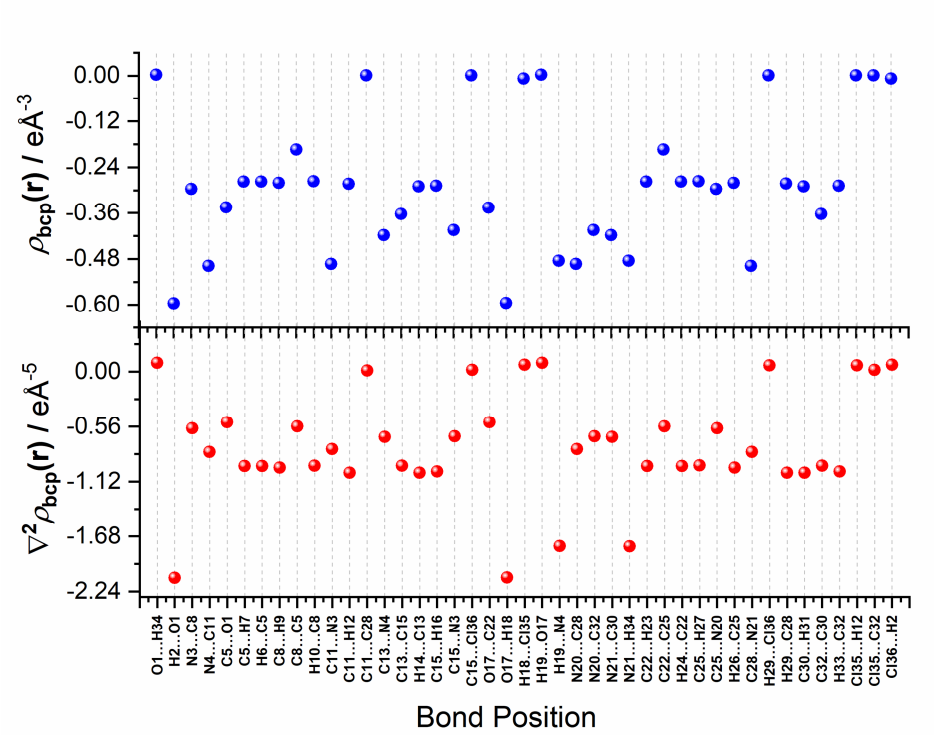

Figure 10. Plot of (**a**) electron density ρ_{bcp}(r) and (**b**) Laplacian of electron density $\nabla^2\rho_{bcp}$ (r) of the dimer of EtOHImCl PIL calculated using the structure optimized at B3LYP/6-311++G(d,p) level of theory. Atom numbering is shown in Figure S2 in Supporting Information.

3.5.2. Electron Localized Function (ELF) and Localized Orbital Locator (LOL) Surface Map Analysis

The electron delocalization in ILs is measured using ELF and LOL surface map analysis. The localisation of electrons at atomic as well as molecular levels is understood using ELF and LOL surface maps [79]. ELF determines the possibility of finding the electrons in the molecular system. It provides the visualisation of both lone-pairs and bond-pairs, which are localised close to interacting atoms. The degree of delocalization of electrons into σ and π components. These functions are intuitive method to understand the chemical bonds. Figure 12a,b show the ELF and LOL plots for the compound EtOHImCl dimer calculated using the structure optimized at B3LYP/6-311++G(d,p) level of theory. The related data has been shown in Figure 11. Figure 12 show the diagrams hav-

ing the separate colour pallets from blue to red. It corresponds to a range from 0.000 to 1.000 for ELF plot whereas the range till 0.800 for LOL plot. The maxima of localization of electron pairs have been found close to covalent bonds while the presence of non-covalent interactions is understood through relative colours. The delocalization of electron is depicted using colours having range below 0.5 while the electron localization is highlighted using colour through range above 0.5. Thus, the light blue is observed in plot is showing the delocalization of electron. Thus, ELF and LOL plots provide the clear picture of interaction present in ion pair of EtOHImCl PIL.

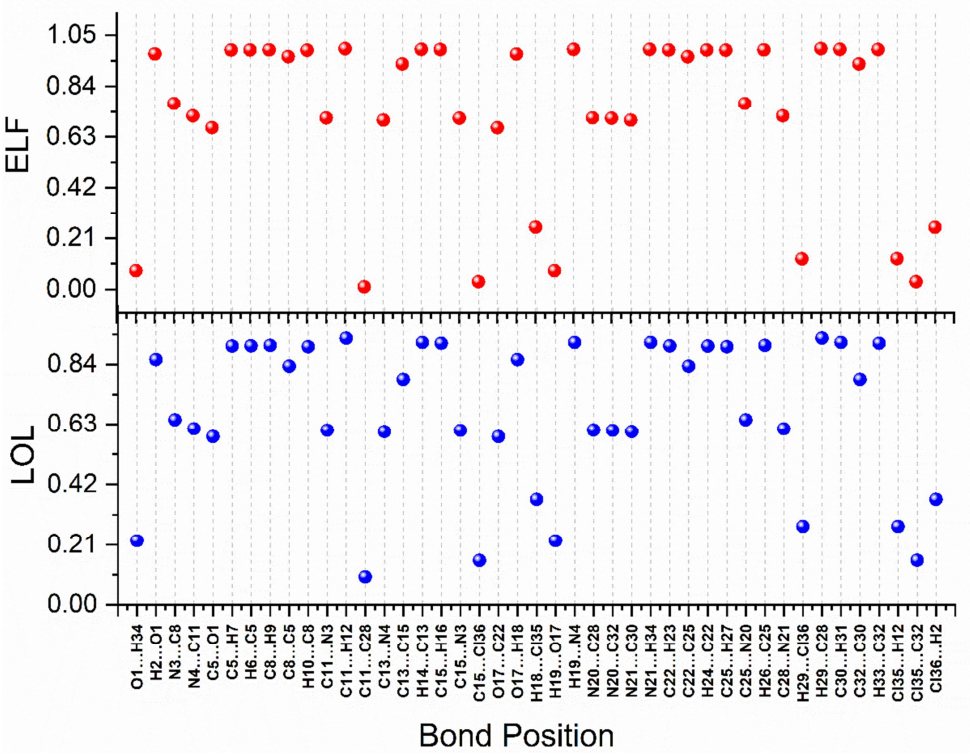

Figure 11. (**a**) ELF and (**b**) LOL data of the dimer of EtOHImCl PIL calculated using the structure optimized at B3LYP/6-311++G(d,p) level of theory. Atom numbering is shown in Figure S2 in Supporting Information.

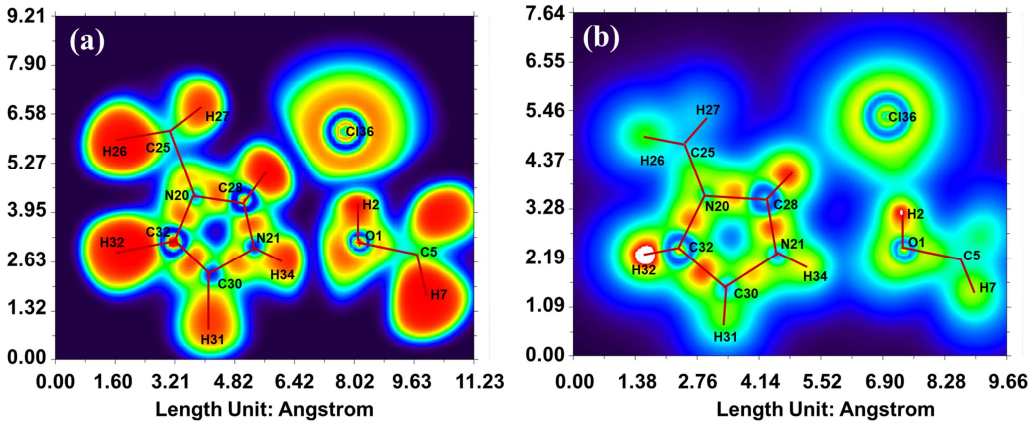

Figure 12. (**a**) ELF and (**b**) LOL analysis of the dimer of EtOHImCl PIL calculated using the structure optimized at B3LYP/6-311++G(d,p) level of theory. Atom numbering is shown in Figure S2 in Supporting Information.

3.6. Non-Covalent Interaction (NCI)

The NCI provides the two-dimensional representation of reduced density gradient (RDG) as well as electron density, which is shown in Figure 13a. Figure 13b represents the isosurface extraction of NCI analysis for the non-covalent interaction present in the dimer of EtOHImCl PIL. The calculation is performed using the optimized geometry at B3LYP/6-311++G** level of theory. The pallet in Figure 13a describes the colour scheme for the plot having λ_2 range from −0.06 (blue) to 0.06 (red). The blue colour shows the most attractive interaction while the red colour indicates the most repulsive forces [80]. The green colour in the plot corresponds to $\lambda_2$equal to zero and represents van der Waals interaction. The blue and green colours in the middle of the plot arises due to hydrogen bonding interaction. Each spike in the plot is originated as a result of specific interaction. The spike in the NCI plot near λ_2 value close to 0.03 represents H-bonding interaction.

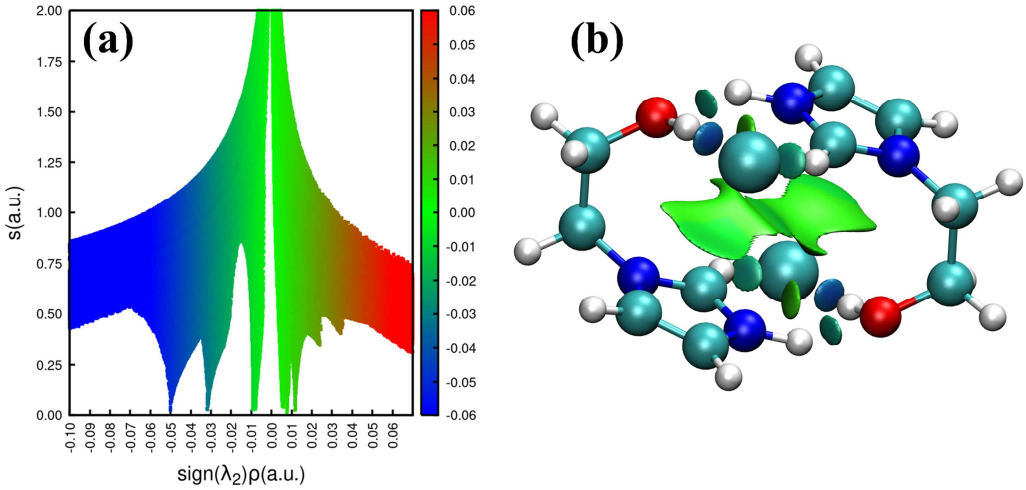

Figure 13. (**a**) RDG plot and (**b**) Isosurface extractions of RDG plots of NCI analysis of the dimer of EtOHImCl PIL calculated using the structure optimized at B3LYP/6-311++G(d,p) level of theory.

3.7. Energy Decomposition Analysis (EDA)

A quantitative interpretation of interactions in the dimer of EtOHImCl IL has been performed using EDA at m05-2x/cc-pVDZ level of theory. Interestingly, the LMO-EDA calculates the total interaction energy is −0.441350 a.u. and the electrostatic, exchange, repulsion, polarisation, and dispersion energies are measured −1110.6428, −167.15, 576.05, −259.91 and −197.11 kJ/mol, respectively [59]. The electrostatic contribution is found nearly five times of dispersion interaction, which dictates that the mainly the IL is mainly stabilized electrostatically. The dispersion component is measured ~17% of total interaction energy. The contributing interaction to hold the IL are mainly N-H…O, C-H…Cl, and O-H…Cl interactions.

3.8. Ab Initio Molecular Dynamics (AIMD) Assay

The molecular dynamics using the AIMD assay is performed at the finite temperature dynamics trajectories to evaluate microscopic mechanics [76,81]. The computation is done using forces computed “on the fly” through electronic structure quantum calculation. The AIMD simulations of dimer of EtOHImCl PIL has been performed at initial temperature of 350 K using time step of 0.5 fs by applying the Timecon of 10.0 fs. The AIMD study of 500 fs is reported in Figure 14. Figure 14a represent the total energy of IL during the AIMD simulation of dimer of EtOHImCl PIL, where the maximum energy of −1680.6068 a.u. close to 237 fs. The relative low energy of −1680.6510 a.u. during the AIMD calculation has been observed close to 100 fs as well as 400 fs. Figure 14b depicts the drift change during the molecular dynamics calculations. The change of important

H-bonding interaction such as O1-H2…Cl36, C29-H29…Cl36, C11-H12…Cl35 and O17-H18…Cl35 during AIMD simulation has been reported in Figure 14c. The distance of H2…Cl36 and H29…Cl36 H-bonding interactions varies between 1.72 and 2.11 Å whereas the distance of H12…Cl35 and H18…Cl35 interactions varies between 1.95 and 2.56 Å.

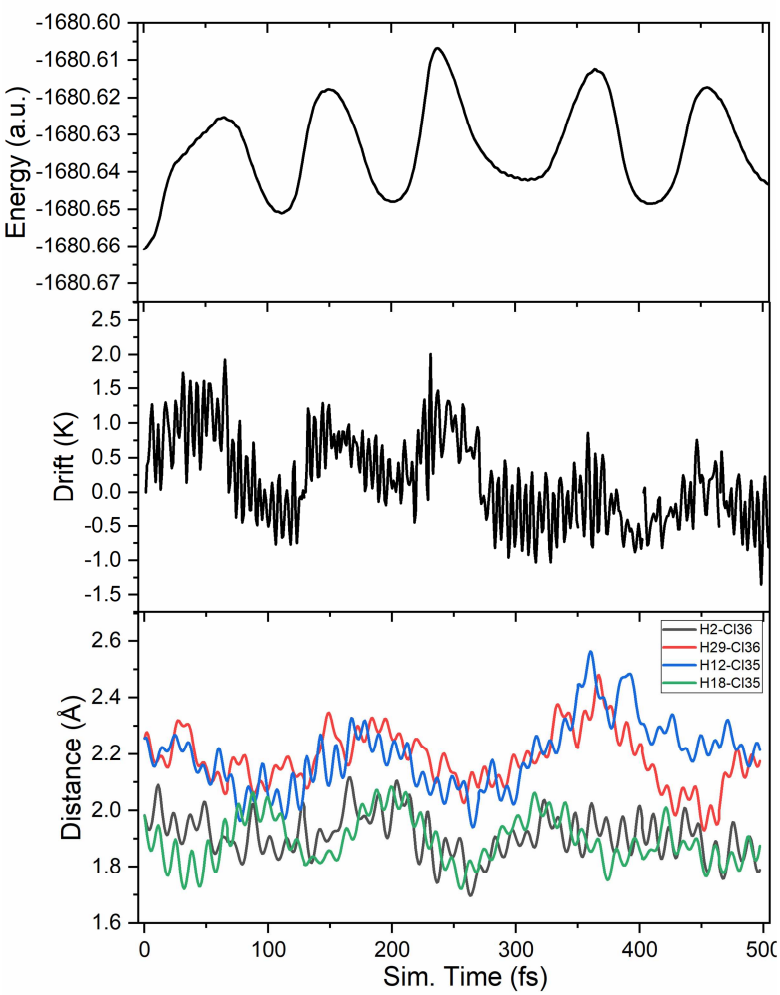

Figure 14. (**a**) Energy (**b**) drift and (**c**) important hydrogen bond distances during AIMD simulations of dimer of EtOHImCl PIL. Atom numbering is shown in Figure S2 in Supporting Information.

4. Conclusions

In this paper, we have investigated the structural properties of hydroxyl functionalized 1*H*-imidazolium Chloride, namely 3-(2-Hydroxyethyl)-1-H-imidazolium chloride (EtOHImCl) by experiments and theoretical results. Here, we are also reporting the effect of theoretically predicted isolated ion-pairs and ion-pair dimers of EtOHImCl on the physical properties of IL. It is also observed that the commonly C_2-H…anion H-bonding interactions is not observed in ion-pair of EtOHImCl. In EtOHImCl, the hydroxyl group of the cation contributes significantly to a H-bond with the Cl anion in ion-pair and dimeric ion-pair of EtOHImCl. When two ion-pairs interacts to each other, it forms dimeric ion-pair with highly interesting H-bonding pattern governed by cation-cation interactions. The hydrogen atom of the OH group interacts with the Cl anion via H-bonding interaction. Further, the oxygen atom of hydroxyl group forms H-bonds along with N-H and Cl anion which is also connected to the C_2-H protons via H-bonding interaction to establish a distinct dimer and so on. These centre H-bonding arrangements result in a 1D

layered molecular structure and promote the stability of the ion-pair dimers. Systematic analytical approach of DFT calculations of isolated ion-pair and dimer has shown its potential for studying the physical chemistry of complex materials. From second order perturbation energy calculation, the strength of O-H…Cl H bonding interaction has been measured ~133.8 kJ/mol. AIMD calculation shows that the relative low energy of −1680.6510 a.u. is found close to 100 fs as well as 400 fs.

Supplementary Materials:.

Author Contributions:.

Funding:

Data Availability Statement:

Acknowledgments: SKP acknowledges to Tarsadia Institute of Chemical Science, Uka Tarsadia University, Surat-394350, Gujrat, India for providing infrastructure as well as instrument facilities. SK thanks Magadh University, Bodh Gaya, Bihar, India for providing lab facility and SERB, Department of Science and Technology (DST), India (Grant No. SRG/2019/002284) for financial support.

Conflicts of Interest: The authors declare no conflict of interest.

References

1. Plechkova, N.V.; Seddon, K.R. Applications of ionic liquids in the chemical industry. *Chemical Society Reviews* **2008**, *37*, 123-150, doi:10.1039/B006677J.
2. Menne, S.; Pires, J.; Anouti, M.; Balducci, A. Protic ionic liquids as electrolytes for lithium-ion batteries. *Electrochemistry Communications* **2013**, *31*, 39-41, doi:https://doi.org/10.1016/j.elecom.2013.02.026.
3. Panja, S.K.; Saha, S. Recyclable, magnetic ionic liquid bmim[FeCl4]-catalyzed, multicomponent, solvent-free, green synthesis of quinazolines. *RSC Advances* **2013**, *3*, 14495-14500, doi:https://doi.org/10.1039/C3RA42039F.
4. Shabashini, A.; Richard, S.; Solanky, T.; Biswas, A.; Kumar, S.; Chandra Nandi, G.; Kumar Panja, S. Effect of dipolar state on J-type aggregation of acceptor group modified pyrene-based push-pull systems. *Journal of Photochemistry and Photobiology A: Chemistry* **2024**, 115971, doi:https://doi.org/10.1016/j.jphotochem.2024.115971.
5. Panja, S.K.; Dwivedi, N.; Noothalapati, H.; Shigeto, S.; Sikder, A.K.; Saha, A.; Sunkari, S.S.; Saha, S. Significance of weak interactions in imidazolium picrate ionic liquids: spectroscopic and theoretical studies for molecular level understanding. *Physical Chemistry Chemical Physics* **2015**, *17*, 18167-18177, doi:https://doi.org/10.1039/C5CP01944C.
6. Jalili, A.H.; Mehdizadeh, A.; Shokouhi, M.; Sakhaeinia, H.; Taghikhani, V. Solubility of CO2 in 1-(2-hydroxyethyl)-3-methylimidazolium ionic liquids with different anions. *The Journal of Chemical Thermodynamics* **2010**, *42*, 787-791, doi:https://doi.org/10.1016/j.jct.2010.02.002.
7. Sun, J.; Zhang, S.; Cheng, W.; Ren, J. Hydroxyl-functionalized ionic liquid: a novel efficient catalyst for chemical fixation of CO2 to cyclic carbonate. *Tetrahedron Letters* **2008**, *49*, 3588-3591, doi:https://doi.org/10.1016/j.tetlet.2008.04.022.
8. Holbrey, J.D.; Turner, M.B.; Reichert, W.M.; Rogers, R.D. New ionic liquids containing an appended hydroxyl functionality from the atom-efficient, one-pot reaction of 1-methylimidazole and acid with propylene oxide. *Green Chemistry* **2003**, *5*, 731-736, doi:10.1039/B311717K.
9. Branco, L.C.; Rosa, J.N.; Moura Ramos, J.J.; Afonso, C.A.M. Preparation and Characterization of New Room Temperature Ionic Liquids. *Chemistry – A European Journal* **2002**, *8*, 3671-3677, doi:https://doi.org/10.1002/1521-3765(20020816)8:16<3671::AID-CHEM3671>3.0.CO;2-9.
10. Recham, N.; Dupont, L.; Courty, M.; Djellab, K.; Larcher, D.; Armand, M.; Tarascon, J.M. Ionothermal Synthesis of Tailor-Made LiFePO4 Powders for Li-Ion Battery Applications. *Chemistry of Materials* **2009**, *21*, 1096-1107, doi:https://doi.org/10.1021/cm803259x.
11. Yang, X.; Fei, Z.; Zhao, D.; Ang, W.H.; Li, Y.; Dyson, P.J. Palladium Nanoparticles Stabilized by an Ionic Polymer and Ionic Liquid: A Versatile System for C−C Cross-Coupling Reactions. *Inorganic Chemistry* **2008**, *47*, 3292-3297, doi:https://doi.org/10.1021/ic702305t.
12. Zhang, S.; Qi, X.; Ma, X.; Lu, L.; Deng, Y. Hydroxyl Ionic Liquids: The Differentiating Effect of Hydroxyl on Polarity due to Ionic Hydrogen Bonds between Hydroxyl and Anions. *The Journal of Physical Chemistry B* **2010**, *114*, 3912-3920, doi:10.1021/jp911430t.

13. Panja, S.K.; Srivastava, N.; Srivastava, J.; Prasad, N.E.; Noothalapati, H.; Shigeto, S.; Saha, S. Evidence of C--F-P and aromatic π--F-P weak interactions in imidazolium ionic liquids and its consequences. *Spectrochimica Acta Part A: Molecular and Biomolecular Spectroscopy* **2018**, *194*, 117-125, doi:https://doi.org/10.1016/j.saa.2017.12.048.
14. Fumino, K.; Reimann, S.; Ludwig, R. Probing molecular interaction in ionic liquids by low frequency spectroscopy: Coulomb energy, hydrogen bonding and dispersion forces. *Physical Chemistry Chemical Physics* **2014**, *16*, 21903-21929, doi:10.1039/C4CP01476F.
15. Niemann, T.; Stange, P.; Strate, A.; Ludwig, R. When hydrogen bonding overcomes Coulomb repulsion: from kinetic to thermodynamic stability of cationic dimers. *Physical Chemistry Chemical Physics* **2019**, *21*, 8215-8220, doi:10.1039/C8CP06417B.
16. Kumar, S.; Das, A. Observation of exclusively π-stacked heterodimer of indole and hexafluorobenzene in the gas phase. *The Journal of Chemical Physics* **2013**, *139*, 104311, doi:https://doi.org/10.1063/1.4820532.
17. Fumino, K.; Peppel, T.; Geppert-Rybczyńska, M.; Zaitsau, D.H.; Lehmann, J.K.; Verevkin, S.P.; Köckerling, M.; Ludwig, R. The influence of hydrogen bonding on the physical properties of ionic liquids. *Physical Chemistry Chemical Physics* **2011**, *13*, 14064-14075, doi:10.1039/C1CP20732F.
18. Fumino, K.; Wulf, A.; Ludwig, R. Strong, Localized, and Directional Hydrogen Bonds Fluidize Ionic Liquids. *Angewandte Chemie International Edition* **2008**, *47*, 8731-8734, doi:https://doi.org/10.1002/anie.200803446.
19. Corderí, S.; González, E.J.; Calvar, N.; Domínguez, Á. Application of [HMim][NTf2], [HMim][TfO] and [BMim][TfO] ionic liquids on the extraction of toluene from alkanes: Effect of the anion and the alkyl chain length of the cation on the LLE. *The Journal of Chemical Thermodynamics* **2012**, *53*, 60-66, doi:https://doi.org/10.1016/j.jct.2012.04.015.
20. Giraud, G.; Gordon, C.M.; Dunkin, I.R.; Wynne, K. The effects of anion and cation substitution on the ultrafast solvent dynamics of ionic liquids: A time-resolved optical Kerr-effect spectroscopic study. *The Journal of Chemical Physics* **2003**, *119*, 464-477, doi:10.1063/1.1578056.
21. Jin, H.; O'Hare, B.; Dong, J.; Arzhantsev, S.; Baker, G.A.; Wishart, J.F.; Benesi, A.J.; Maroncelli, M. Physical Properties of Ionic Liquids Consisting of the 1-Butyl-3-Methylimidazolium Cation with Various Anions and the Bis(trifluoromethylsulfonyl)imide Anion with Various Cations. *The Journal of Physical Chemistry B* **2008**, *112*, 81-92, doi:10.1021/jp076462h.
22. Katsyuba, S.A.; Zvereva, E.E.; Vidiš, A.; Dyson, P.J. Application of Density Functional Theory and Vibrational Spectroscopy Toward the Rational Design of Ionic Liquids. *The Journal of Physical Chemistry A* **2007**, *111*, 352-370, doi:10.1021/jp064610i.
23. Li, Y.; Hu, Y.; Chen, G.; Wang, Z.; Jin, X. Rapid proton diffusion in hydroxyl functionalized imidazolium ionic liquids. *Science China Chemistry* **2017**, *60*, 734-739, doi:https://doi.org/10.1007/s11426-016-0459-2.
24. Wong, C.Y.; Wong, W.Y.; Loh, K.S.; Lim, K.L. Protic ionic liquids as next-generation proton exchange membrane materials: Current status & future perspectives. *Reactive and Functional Polymers* **2022**, *171*, 105160, doi:https://doi.org/10.1016/j.reactfunctpolym.2022.105160.
25. Johansson, K.M.; Izgorodina, E.I.; Forsyth, M.; MacFarlane, D.R.; Seddon, K.R. Protic ionic liquids based on the dimeric and oligomeric anions: [(AcO)xHx−1]−. *Physical Chemistry Chemical Physics* **2008**, *10*, 2972-2978, doi:https://doi.org/10.1039/B801405A.
26. Enomoto, T.; Nakamori, Y.; Matsumoto, K.; Hagiwara, R. Ion−Ion Interactions and Conduction Mechanism of Highly Conductive Fluorohydrogenate Ionic Liquids. *The Journal of Physical Chemistry C* **2011**, *115*, 4324-4332, doi:10.1021/jp1101219.
27. Keutsch, F.N.; Saykally, R.J. Water clusters: Untangling the mysteries of the liquid, one molecule at a time. *Proceedings of the National Academy of Sciences* **2001**, *98*, 10533-10540, doi:https://doi.org/10.1073/pnas.191266498.
28. Ludwig, R. Water: From Clusters to the Bulk. *Angewandte Chemie International Edition* **2001**, *40*, 1808-1827, doi:https://doi.org/10.1002/1521-3773(20010518)40:10<1808::AID-ANIE1808>3.0.CO;2-1.
29. Huisken, F.; Stemmler, M. Infrared photodissociation of small methanol clusters. *Chemical Physics Letters* **1988**, *144*, 391-395, doi:https://doi.org/10.1016/0009-2614(88)87135-5.
30. Panja, S.K.; Haddad, B.; Debdab, M.; Kiefer, J.; Chaker, Y.; Bresson, S.; Paolone, A. Cluster Formation through Hydrogen Bond Bridges across Chloride Anions in a Hydroxyl-Functionalized Ionic Liquid. *ChemPhysChem* **2019**, *20*, 936-940, doi:https://doi.org/10.1002/cphc.201801206.
31. Niemann, T.; Strate, A.; Ludwig, R.; Zeng, H.J.; Menges, F.S.; Johnson, M.A. Spectroscopic Evidence for an Attractive Cation–Cation Interaction in Hydroxy-Functionalized Ionic Liquids: A Hydrogen-Bonded Chain-like Trimer. *Angewandte Chemie International Edition* **2018**, *57*, 15364-15368, doi:https://doi.org/10.1002/anie.201808381.
32. Menges, F.S.; Zeng, H.J.; Kelleher, P.J.; Gorlova, O.; Johnson, M.A.; Niemann, T.; Strate, A.; Ludwig, R. Structural Motifs in Cold Ternary Ion Complexes of Hydroxyl-Functionalized Ionic Liquids: Isolating the Role of Cation–Cation Interactions. *The Journal of Physical Chemistry Letters* **2018**, *9*, 2979-2984, doi:https://doi.org/10.1021/acs.jpclett.8b01130.

33. Thummuru, D.N.R.; Mallik, B.S. Structure and Dynamics of Hydroxyl-Functionalized Protic Ammonium Carboxylate Ionic Liquids. *The Journal of Physical Chemistry A* **2017**, *121*, 8097-8107, doi:https://doi.org/10.1021/acs.jpca.7b05995.
34. Fakhraee, M.; Zandkarimi, B.; Salari, H.; Gholami, M.R. Hydroxyl-Functionalized 1-(2-Hydroxyethyl)-3-methyl Imidazolium Ionic Liquids: Thermodynamic and Structural Properties using Molecular Dynamics Simulations and ab Initio Calculations. *The Journal of Physical Chemistry B* **2014**, *118*, 14410-14428, doi:10.1021/jp5083714.
35. Panja, S.K.; Haddad, B.; Kiefer, J. Clusters of the Ionic Liquid 1-Hydroxyethyl-3-methylimidazolium Picrate: From Theoretical Prediction in the Gas Phase to Experimental Evidence in the Solid State. *ChemPhysChem* **2018**, *19*, 3061-3068, doi:https://doi.org/10.1002/cphc.201800684.
36. Knorr, A.; Ludwig, R. Cation-cation clusters in ionic liquids: Cooperative hydrogen bonding overcomes like-charge repulsion. *Scientific Reports* **2015**, *5*, 17505, doi:https://doi.org/10.1038/srep17505.
37. Knorr, A.; Stange, P.; Fumino, K.; Weinhold, F.; Ludwig, R. Spectroscopic Evidence for Clusters of Like-Charged Ions in Ionic Liquids Stabilized by Cooperative Hydrogen Bonding. *ChemPhysChem* **2016**, *17*, 458-462, doi:https://doi.org/10.1002/cphc.201501134.
38. Strate, A.; Niemann, T.; Michalik, D.; Ludwig, R. When Like Charged Ions Attract in Ionic Liquids: Controlling the Formation of Cationic Clusters by the Interaction Strength of the Counterions. *Angewandte Chemie International Edition* **2017**, *56*, 496-500, doi:https://doi.org/10.1002/anie.201609799.
39. Niemann, T.; Zaitsau, D.; Strate, A.; Villinger, A.; Ludwig, R. Cationic clustering influences the phase behaviour of ionic liquids. *Scientific Reports* **2018**, *8*, 14753, doi:10.1038/s41598-018-33176-6.
40. Morais, E.M.; Abdurrokhman, I.; Martinelli, A. Solvent-free synthesis of protic ionic liquids. Synthesis, characterization and computational studies of triazolium based ionic liquids. *Journal of Molecular Liquids* **2022**, *360*, 119358, doi:https://doi.org/10.1016/j.molliq.2022.119358.
41. Lee, C.; Yang, W.; Parr, R.G. Development of the Colle-Salvetti correlation-energy formula into a functional of the electron density. *Physical review B* **1988**, *37*, 785.
42. Becke, A. Density-functional thermochemistry. III. The role of exact exchange Ab initio effective core potentials for molecular calculations. Potentials for K to Au including the outermost core orbitals Self-consistent molecular orbital methods. XX. A basis set for. *J. Chem. Phys. J. Chem. Phys. J. Chem. Phys. J. Chem. Phys. Hg J. Chem. Phys. J. Chem. Phys. J. Chem. Phys* **1993**, *981*, 448799-449982.
43. Miehlich, B.; Savin, A.; Stoll, H.; Preuss, H. Results obtained with the correlation energy density functionals of Becke and Lee, Yang and Parr. *Chemical Physics Letters* **1989**, *157*, 200-206.
44. McLean, A.D.; Chandler, G.S. Contracted Gaussian basis sets for molecular calculations. I. Second row atoms, Z=11–18. *The Journal of Chemical Physics* **1980**, *72*, 5639-5648, doi:10.1063/1.438980.
45. Krishnan, R.; Binkley, J.S.; Seeger, R.; Pople, J.A. Self-consistent molecular orbital methods. XX. A basis set for correlated wave functions. *The Journal of Chemical Physics* **1980**, *72*, 650-654, doi:10.1063/1.438955.
46. M. J. Frisch, G., Revision A.02, Gaussian Inc., Wallingford CT, 2016.
47. Jamróz, M.H. Vibrational Energy Distribution Analysis (VEDA): Scopes and limitations. *Spectrochimica Acta Part A: Molecular and Biomolecular Spectroscopy* **2013**, *114*, 220-230, doi:https://doi.org/10.1016/j.saa.2013.05.096.
48. Kempter, V.; Kirchner, B. The role of hydrogen atoms in interactions involving imidazolium-based ionic liquids. *Journal of Molecular Structure* **2010**, *972*, 22-34, doi:https://doi.org/10.1016/j.molstruc.2010.02.003.
49. Boys, S.F.; Bernardi, F. The calculation of small molecular interactions by the differences of separate total energies. Some procedures with reduced errors. *Molecular Physics* **1970**, *19*, 553-566, doi:https://doi.org/10.1080/00268977000101561.
50. Simon, S.; Duran, M.; Dannenberg, J.J. How does basis set superposition error change the potential surfaces for hydrogen-bonded dimers? *The Journal of Chemical Physics* **1996**, *105*, 11024-11031, doi:10.1063/1.472902.
51. Kumar, S. Curcumin as a potential multiple-target inhibitor against SARS- ip CoV-2 Infection: A detailed interaction study using quantum chemical calculations. *Journal of the Serbian Chemical Society* **2022**, doi:https://doi.org/10.2298/JSC220921087K.
52. Kumar, S.; Das, A. Mimicking trimeric interactions in the aromatic side chains of the proteins: A gas phase study of indole[ellipsis (horizontal)](pyrrole)2 heterotrimer. *The Journal of Chemical Physics* **2012**, *136*, 174302, doi:https://doi.org/10.1063/1.4706517.
53. Kumar, S.; Kaul, I.; Biswas, P.; Das, A. Structure of 7-Azaindole···2-Fluoropyridine Dimer in a Supersonic Jet: Competition between N–H···N and N–H···F Interactions. *The Journal of Physical Chemistry A* **2011**, *115*, 10299-10308, doi:https://doi.org/10.1021/jp205894q.
54. Kumar, S.; Singh, S.K.; Vaishnav, J.K.; Hill, J.G.; Das, A. Interplay among Electrostatic, Dispersion, and Steric Interactions: Spectroscopy and Quantum Chemical Calculations of π-Hydrogen Bonded Complexes. *ChemPhysChem* **2017**, *18*, 828-838, doi:https://doi.org/10.1002/cphc.201601405.

55. Singh, S.K.; Kumar, S.; Das, A. Competition between n →π*(Ar) and conventional hydrogen bonding (N–H···N) interactions: an ab initio study of the complexes of 7-azaindole and fluorosubstituted pyridines. *Phys. Chem. Chem. Phys.* **2014**, *16*, 8819-8827, doi:https://doi.org/10.1039/C3CP54169J.
56. Kumar, S.; Pande, V.; Das, A. π-Hydrogen Bonding Wins over Conventional Hydrogen Bonding Interaction: A Jet-Cooled Study of Indole···Furan Heterodimer. *The Journal of Physical Chemistry A* **2012**, *116*, 1368-1374, doi:https://doi.org/10.1021/jp211366z.
57. Kumar, S.; Mukherjee, A.; Das, A. Structure of Indole···Imidazole Heterodimer in a Supersonic Jet: A Gas Phase Study on the Interaction between the Aromatic Side Chains of Tryptophan and Histidine Residues in Proteins. *The Journal of Physical Chemistry A* **2012**, *116*, 11573-11580, doi:https://doi.org/10.1021/jp309167a.
58. Kumar, S.; Das, A. Effect of acceptor heteroatoms on π-hydrogen bonding interactions: A study of indole···thiophene heterodimer in a supersonic jet. *The Journal of Chemical Physics* **2012**, *137*, 094309, doi:https://doi.org/10.1063/1.4748818.
59. Su, P.; Li, H. Energy decomposition analysis of covalent bonds and intermolecular interactions. *The Journal of Chemical Physics* **2009**, *131*, 014102, doi:10.1063/1.3159673.
60. Lu, T.; Chen, F. Multiwfn: A multifunctional wavefunction analyzer. *Journal of Computational Chemistry* **2012**, *33*, 580-592, doi:https://doi.org/10.1002/jcc.22885.
61. Contreras-García, J.; Johnson, E.R.; Keinan, S.; Chaudret, R.; Piquemal, J.-P.; Beratan, D.N.; Yang, W. NCIPLOT: A Program for Plotting Noncovalent Interaction Regions. *Journal of Chemical Theory and Computation* **2011**, *7*, 625-632, doi:https://doi.org/10.1021/ct100641a.
62. Neese, F. The ORCA program system. *Wiley Interdisciplinary Reviews: Computational Molecular Science* **2012**, *2*, 73-78, doi:https://doi.org/10.1002/wcms.81.
63. Paschoal, V.H.; Faria, L.F.O.; Ribeiro, M.C.C. Vibrational Spectroscopy of Ionic Liquids. *Chemical Reviews* **2017**, *117*, 7053-7112, doi:https://doi.org/10.1021/acs.chemrev.6b00461.
64. Khudozhitkov, A.E.; Neumann, J.; Niemann, T.; Zaitsau, D.; Stange, P.; Paschek, D.; Stepanov, A.G.; Kolokolov, D.I.; Ludwig, R. Hydrogen Bonding Between Ions of Like Charge in Ionic Liquids Characterized by NMR Deuteron Quadrupole Coupling Constants—Comparison with Salt Bridges and Molecular Systems. *Angewandte Chemie International Edition* **2019**, *58*, 17863-17871, doi:https://doi.org/10.1002/anie.201912476.
65. Kiefer, J.; Wagenfeld, S.; Kerlé, D. Chain length effects on the vibrational structure and molecular interactions in the liquid normal alkyl alcohols. *Spectrochimica Acta Part A: Molecular and Biomolecular Spectroscopy* **2018**, *189*, 57-65, doi:https://doi.org/10.1016/j.saa.2017.07.061.
66. Schmidt, D.A.; Miki, K. Structural Correlations in Liquid Water: A New Interpretation of IR Spectroscopy. *The Journal of Physical Chemistry A* **2007**, *111*, 10119-10122, doi:10.1021/jp074737n.
67. Kumar, S.; Biswas, P.; Kaul, I.; Das, A. Competition between Hydrogen Bonding and Dispersion Interactions in the Indole···Pyridine Dimer and (Indole) ₂ ···Pyridine Trimer Studied in a Supersonic Jet. *The Journal of Physical Chemistry A* **2011**, *115*, 7461-7472, doi:https://doi.org/10.1021/jp202658r.
68. Kumar, S.; Singh, S.K.; Calabrese, C.; Maris, A.; Melandri, S.; Das, A. Structure of saligenin: microwave, UV and IR spectroscopy studies in a supersonic jet combined with quantum chemistry calculations. *Physical Chemistry Chemical Physics* **2014**, *16*, 17163, doi:https://doi.org/10.1039/C4CP01693A.
69. Sada, P.K.; Bar, A.; Jassal, A.K.; Kumar, P.; Srikrishna, S.; Singh, A.K.; Kumar, S.; Singh, L.; Rai, A. A Novel Rhodamine Probe Acting as Chemosensor for Selective Recognition of Cu2+ and Hg2+ Ions: An Experimental and First Principle Studies. *Journal of Fluorescence* **2023**, doi:https://doi.org/10.1007/s10895-023-03412-y.
70. Kiefer, J.; Pye, C.C. Structure of the Room-Temperature Ionic Liquid 1-Hexyl-3-methylimidazolium Hydrogen Sulfate: Conformational Isomerism. *The Journal of Physical Chemistry A* **2010**, *114*, 6713-6720, doi:10.1021/jp1031527.
71. Wulf, A.; Fumino, K.; Ludwig, R. Comment on "New Interpretation of the CH Stretching Vibrations in Imidazolium-Based Ionic Liquids". *The Journal of Physical Chemistry A* **2010**, *114*, 685-686, doi:10.1021/jp9080146.
72. Grondin, J.; Lassègues, J.-C.; Cavagnat, D.; Buffeteau, T.; Johansson, P.; Holomb, R. Revisited vibrational assignments of imidazolium-based ionic liquids. *Journal of Raman Spectroscopy* **2011**, *42*, 733-743, doi:https://doi.org/10.1002/jrs.2754.
73. Andersson, M.P.; Uvdal, P. New Scale Factors for Harmonic Vibrational Frequencies Using the B3LYP Density Functional Method with the Triple-ζ Basis Set 6-311+G(d,p). *The Journal of Physical Chemistry A* **2005**, *109*, 2937-2941, doi:10.1021/jp045733a.
74. Hamaguchi, H.-O.; Ozawa, R. Structure of Ionic Liquids and Ionic Liquid Compounds: Are Ionic Liquids Genuine Liquids in the Conventional Sense? In *Advances in Chemical Physics*; Advances in Chemical Physics; 2005; pp. 85-104.
75. Ozawa, R.; Hayashi, S.; Saha, S.; Kobayashi, A.; Hamaguchi, H.-o. Rotational Isomerism and Structure of the 1-Butyl-3-methylimidazolium Cation in the Ionic Liquid State. *Chemistry Letters* **2003**, *32*, 948-949, doi:https://doi.org/10.1246/cl.2003.948.

76. Kumar Panja, S.; Kumar, S. Weak intra and intermolecular interactions via aliphatic hydrogen bonding in piperidinium based ionic Liquids: Experimental, topological and molecular dynamics studies. *Journal of Molecular Liquids* **2023**, *375*, 121354, doi:https://doi.org/10.1016/j.molliq.2023.121354.
77. NBO 7.0. E. D. Glendening, J., K. Badenhoop, A. E. Reed, J. E. Carpenter, J. A. Bohmann, C. M. Morales, P. Karafiloglou, C. R. Landis, and F. Weinhold, Theoretical Chemistry Institute, University of Wisconsin, Madison (2018).
78. Kumar, V.; Kumar, R.; Kumar, N.; Kumar, S. Solvation Dynamics of Oxadiazoles as Potential Candidate for Drug Preparation. *Asian J. Chem.* **2023**, *35*, doi:https://doi.org/10.14233/ajchem.2023.27594.
79. Prasana, J.C.; Muthu, S.; Abraham, C.S. Molecular docking studies, charge transfer excitation and wave function analyses (ESP, ELF, LOL) on valacyclovir: a potential antiviral drug. *Computational biology and chemistry* **2019**, *78*, 9-17.
80. Kumar, S.; Panja, S.K. Intermolecular charge-transfer complex between solute and ionic liquid: experimental and theoretical studies. *Theoretical Chemistry Accounts* **2023**, *142*, 126, doi:https://doi.org/10.1007/s00214-023-03073-x.
81. Kumar Panja, S.; Kumar, S.; Fazal, A.D.; Bera, S. Molecular aggregation kinetics of Heteropolyene: An Experimental, topological and solvation dynamics studies. *Journal of Photochemistry and Photobiology A: Chemistry* **2023**, *445*, 115084, doi:https://doi.org/10.1016/j.jphotochem.2023.115084.